The Astrophysical Journal, 744:165 (5pp), 2012 January 10 doi:10.1088/0004-637X/744/2/165

HIGH ANGULAR RESOLUTION RADIO OBSERVATIONS OF A CORONAL MASS EJECTION SOURCE REGION AT LOW FREQUENCIES DURING A SOLAR ECLIPSE

R. Ramesh, C. Kathiravan, Indrajit V. Barve, and M. Rajalingam
Indian Institute of Astrophysics, Bangalore 560 034, India; ramesh@iiap.res.in, kathir@iiap.res.in, indrajit@iiap.res.in, rajalingam@iiap.res.in
Received 2011 July 24; accepted 2011 September 24; published 2011 December 22

ABSTRACT

We carried out radio observations of the solar corona in the frequency range 109–50 MHz during the annular eclipse of 2010 January 15 from the Gauribidanur Observatory, located about 100 km north of Bangalore in India. The radio emission in the above frequency range originates typically in the radial distance range ≈1.2–1.5 $R_\odot$ in the "undisturbed" solar atmosphere. Our analysis indicates that (1) the angular size of the smallest observable radio source (associated with a coronal mass ejection in the present case) is $\approx 1' \pm 0'.3$, (2) the source size does not vary with radial distance, (3) the peak brightness temperature of the source corresponding to the above size at a typical frequency like 77 MHz is $\approx 3 \times 10^9$ K, and (4) the coronal magnetic field near the source region is ≈70 mG.

Key words: eclipses – Sun: corona – Sun: coronal mass ejections (CMEs) – Sun: magnetic topology – Sun: radio radiation – techniques: high angular resolution

1. INTRODUCTION

During a solar eclipse, discrete radio sources on the Sun can be identified with high angular resolution ($\sim 10''$) using the diffraction effects at the Moon's sharp limb (Cohen 1969; Hazard 1976). The limiting resolution is

$$\theta = 2.4 \times 10^9 (1/\nu D)^{1/2} \text{arcsec}, \quad (1)$$

where ν (Hz) is the frequency of observation and D ($\approx 3.8 \times 10^8$ m) is the Earth–Moon distance. One can notice that θ is independent of the size of the radio antenna or the antenna array, which is one of the important factors that restricts the angular resolution in routine observations. Taking advantage of this, we have made an attempt to observe small-sized radio sources in the solar atmosphere from where low-frequency radiation ($\lesssim$100 MHz) originates. Observations during a solar eclipse, particularly at frequencies $\lesssim$100 MHz, are a useful tool to look for small-sized discrete radio sources in the solar atmosphere since the angular resolution of the corresponding radio antenna arrays has always been relatively low. In regard to this connection, we would like to point out that one of the scientific goals of the proposed/upcoming large radio antenna arrays such as LOFAR, FASR, and the Long Wavelength Array is to probe the solar corona with high angular resolution at low frequencies (see, e.g., White et al. 2003; Bastian 2004; Kassim et al. 2005). The motivations for the present work are the following: (1) indications from white light coronagraph observations that structures of angular dimension $\approx 0'.5$ are present at coronal heights where 75 MHz radiation is expected (Gergely 1986); (2) observations with the Culgoora and Clark Lake Radioheliographs, which indicate that there could be discrete coronal radio sources with angular sizes lower than their resolution limit, $\approx 4'$ at 80 and 73.8 MHz, respectively (Kai 1985; Gergely 1986); (3) recent reports suggesting that a maximum angular resolution of $\approx 3'$ may be sufficient for imaging the solar corona at a typical frequency like 100 MHz (Bastian 2004; Cairns 2004); (4) scattering of radio radiation by small-scale density inhomogeneities in the solar corona, and the limiting coronal radio source sizes (Riddle 1974; Kerdraon 1979; Robinson 1983; Lang & Willson 1987; Bastian 1994, 1995; Ramesh & Sastry 2000; Mercier et al. 2006; Kathiravan et al. 2011; Subramanian & Cairns 2011); and (5) though eclipse observations provide the required angular resolution to understand the above issues, the method has not been exploited (Denisse et al. 1952; Ramesh et al. 1999; Kathiravan et al. 2011).

2. OBSERVATIONS

The solar eclipse of 2010 January 15 was partial at the Gauribidanur Observatory (latitude: 13°36′ N; longitude: 77°26′ E)[1] with a magnitude of ≈81% and an obscuration of ≈74%.[2] Note that the solar eclipses are always partial/annular at radio frequencies since the size of the radio Sun is large compared with the Moon. The first contact of the Moon with the "optical" Sun on 2010 January 15 occurred at ≈05:47 UT. The position angle (P.A., measured counterclockwise from the zenith point of the solar disk) of the Moon with respect to the Sun at that time was ≈231°. The corresponding values for the maximum phase of the eclipse were ≈07:53 UT and ≈146°, respectively. The fourth contact was at ≈09:41 UT and P.A. ≈64°. We carried out observations of the solar corona at 77 MHz with the Gauribidanur radioheliograph (GRH; Ramesh et al. 1998) in the imaging mode and over the 109–50 MHz band in the total power mode (Kraus 1966) with the Gauribidanur radio spectrograph system (GRASS; Ebenezer et al. 2007) on the eclipse day. While the GRH has an angular resolution of $\approx 10' \times 15'$ (R.A. × decl.) at 77 MHz, the half-power width of the response of GRASS is $\approx 90^\circ \times 5^\circ$ (R.A. × decl.) at 109 MHz. The width of the response of GRASS in hour angle is nearly independent of frequency. The Sun is a point source for GRASS. The antennas of both GRH and GRASS are fixed vertically pointing toward the zenith. The tilting/steering of the antenna response ("beam") is achieved electronically through the use of diode switches and cable delays in the radio frequency signal path from the antennas. While the GRH has a provision to steer the "beam" in both hour angle and declination, it is only in declination for GRASS. Even in the case of GRH, the provision to tilt the "beam" in hour angle is limited in comparison with the declination. For a bandwidth of ≈1 MHz and integration time ≈1 s, the minimum detectable

[1] http://www.iiap.res.in/centers/radio
[2] http://xjubier.free.fr/site_pages/SolarEclipseCalc_Diagram.html

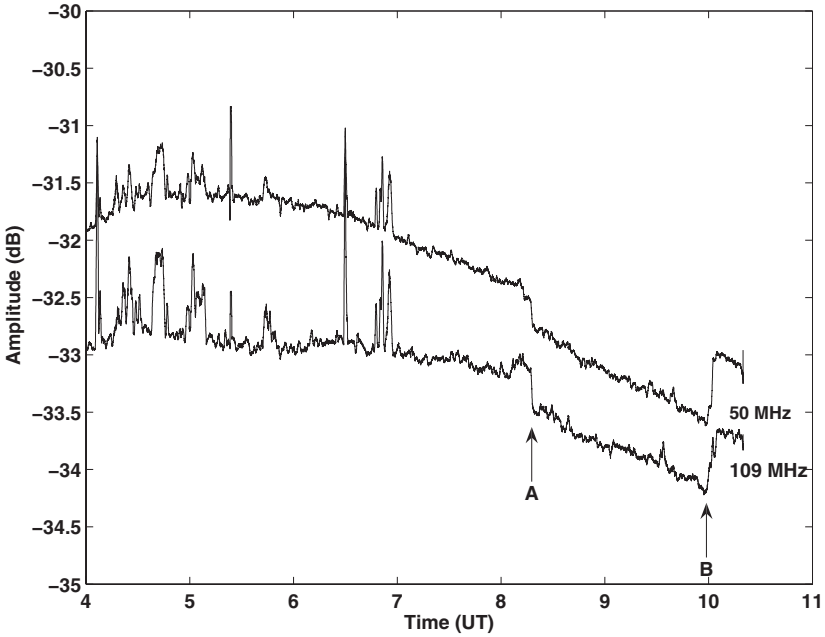

Figure 1. Time profile of the radio emission from the solar corona at 50 and 109 MHz observed on 2010 January 15 with the radio spectrograph at the Gauribidanur Observatory. The "dip" during the time interval ≈08:17–09:59 UT (indicated by arrows A and B) corresponds to the occultation of the discrete radio source mentioned in the text. The integration time used was ≈1 s.

flux density with GRASS is ≈0.1 sfu (sfu = solar flux unit = 10^{-22} W m^{-2} Hz^{-1}). For GRH, it is ≈0.01 sfu.

Since the antennas in GRASS do not track the Sun in hour angle, a plot of the time profile of the observations is the east–west response pattern of the antenna system as the Sun drifts across. The amplitude of each data point is proportional to the strength of the emission from the whole Sun and the Galactic background, multiplied by the antenna gain in that direction. The relative contribution from the Galactic background varies with the local sidereal time and can be significant during the December–January period when the Sun is close to the Galactic center. Note that the R.A. and decl. of the Sun on 2010 January 15 were $19^h47^m30^s$ and $-21\overset{\circ}{.}14$, respectively. The corresponding values for the Galactic center (i.e., Sagittarius A), the strongest source close to the Sun on the aforementioned date, are $17^h42^m30^s$ and $-28\overset{\circ}{.}9$ (1950.0 epoch). A comparison of the positions of the Sun and Sagittarius A indicates that when the "beam" of GRASS is pointed at the Sun, the contribution from Sagittarius A is expected to be lower by $\gtrsim$50% since the latter lies close to the half-power level of the "beam."

In Figure 1, we present the GRASS observations at 50 and 109 MHz (the extreme frequencies of observation) on 2010 January 15 during the interval ≈4:00–10:20 UT. The observed time profiles at both of the above frequencies are consistent with each other. The time profiles at other frequencies in the 50–109 MHz band were also found to be similar. As mentioned earlier, the antennas were kept fixed pointing toward the zenith, so the decrease in the amplitude as a function of time represents the change in the antenna gain with the zenith angle. The "spikes" during the interval 04:00–07:00 UT are most likely transient, weak, type III radio burst emission. The similarity in the emission at two different observing frequencies (50 and 109 MHz) indicates this. Their occurrence during the early phase (≈04:00–07:00 UT) of the soft X-ray flare shown in Figure 2 during which there is a gradual increase in the flare intensity

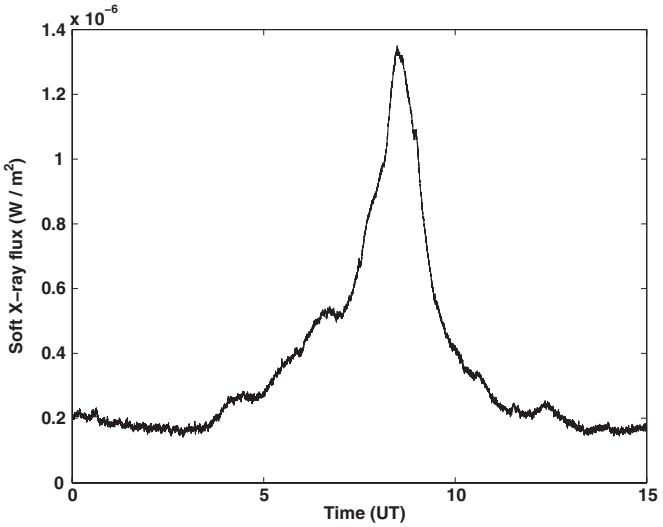

Figure 2. Soft X-ray (0.5–8 Å) emission observed from the whole Sun during the interval 00:00–15:00 UT on 2010 January 15 with the X-ray sensor on board *GOES 14*. The integration time is ≈2 s.

is suggestive of weak electron acceleration/pre-flare heating in the associated region (Kane et al. 1974). The absence of type III bursts close to the impulsive and peak phase (≈07:00–09:00 UT) of the flare indicates that the related reconnection site(s) might be limited to low altitudes in the solar atmosphere. The presence of enhanced X-ray emission alone without radio bursts at low frequencies (which originate at higher altitudes) is in support of this argument (Benz et al. 2005). The flare was of C1.3 class with a peak at 08:41 UT observed with the X-ray sensor on board *GOES 14*. The associated active region was AR 11040 (N30 W29).[3] The "dip" during ≈08:17–09:59 UT in both the

[3] http://www.swpc.noaa.gov

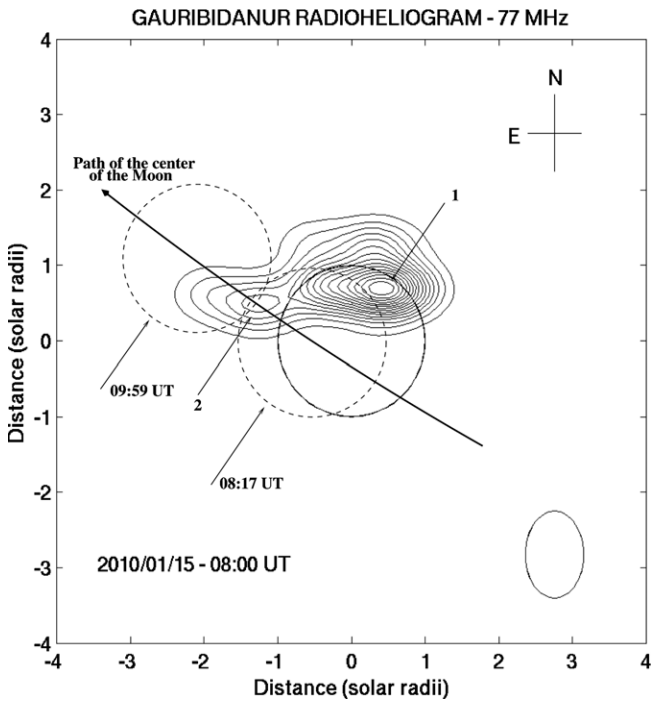

Figure 3. Radioheliogram obtained with GRH on 2010 January 15 at ≈08:00 UT. The circle (drawn with a solid line) at the center indicates the limb of the solar photosphere. The GRH "beam" at 77 MHz is shown near the lower right in the figure. The arrow line is the path of the center of the Moon on 2010 January 15. The "dashed" circles marked 08:17 UT and 09:59 UT are the locations of the Moon on that day at the corresponding epochs. These locations correspond to arrows A and B in Figure 1. The peak T_b is $\approx 7 \times 10^7$ K, corresponding to the discrete source on the disk in the northwest quadrant (indicated by arrow 1). The T_b of the source above the limb in the northeast quadrant is $\approx 2 \times 10^7$ K (indicated by arrow 2).

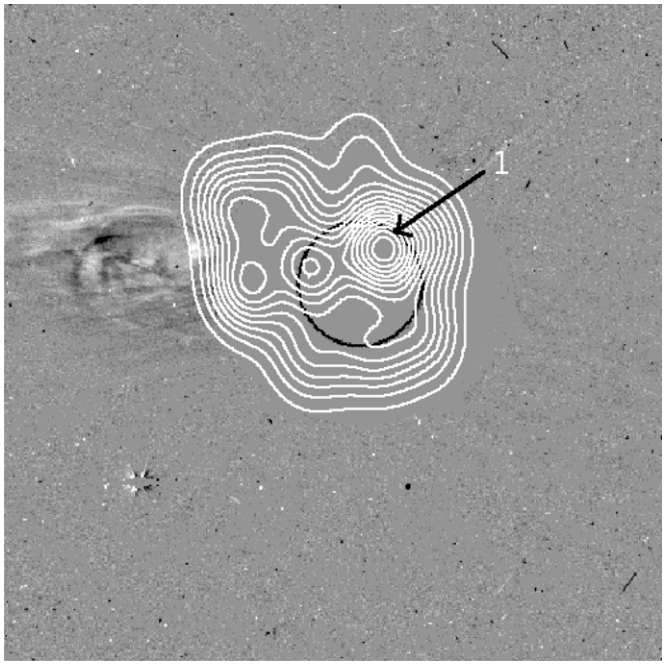

Figure 4. Composite of the radioheliogram (shown in white contours) obtained with GRH at ≈05:00 UT and the *SOHO*-LASCO C2 image at 05:19 UT on 2010 January 15. The inner black circle at the center represents the limb of the solar photosphere, and the concentric, outer gray circle corresponds to the occulting disk of the coronagraph (radius $\approx 2.2\ R_\odot$). Solar north is straight up, and east is to the left. The peak T_b in the radioheliogram is $\approx 1.3 \times 10^6$ K, corresponding to the discrete source close to the limb in the northwest quadrant (indicated by arrow 1).

50 and 109 MHz time profiles (indicated by the arrows A and B, respectively) in Figure 1 is the subject of the present work. We will describe this in more detail in Section 3.

Figure 3 shows the radioheliogram obtained with GRH at ≈08:00 UT on 2010 January 15. The frequency of observation was 77 MHz. The data were calibrated using observations on Cygnus A (3c405), which is a point source for GRH. The peak brightness temperature (T_b) of the source in the northwest quadrant in Figure 3 is $\approx 7 \times 10^7$ K. For the source above the limb in the northeast quadrant, the T_b is $\approx 2 \times 10^7$ K. Other than these two sources, radio emission from elsewhere on the disk and beyond the limb is not noticeable. Some reasons for this could be the high T_b of the above two sources as compared with the background corona, whose T_b is $\approx 10^6$ K, and the limited dynamic range (<20 dB) of the GRH (particularly for observations away from the zenith owing to the use of the cable delay system mentioned earlier). Figure 4 shows the composite of the radioheliogram at 77 MHz obtained with GRH around 05:00 UT on 2010 January 15 and the white light picture of the solar corona taken with LASCO (Brueckner et al. 1995) C2 on board *SOHO* at ≈05:19 UT. The enhanced emission above the east limb in the *SOHO*-LASCO C2 image corresponds to coronal mass ejection (CME) activity.[4] The bulgings in the GRH radio contours above the east limb coincide well with the aforementioned white light emission. The peak T_b in the radioheliogram is $\approx 1.3 \times 10^6$ K, corresponding to the discrete source in the northwest quadrant. This is of the same order as the T_b of the background corona mentioned above. Thus we are able to observe radio emission from all over the corona as in Figure 3. Note that as a result of the limited tracking capability of GRH as mentioned earlier, we were not in a position to obtain a time sequence of images. The increase in the T_b of the discrete radio source in the northwest quadrant at 08:00 UT (Figure 3) as compared with 05:00 UT (Figure 4) is most likely related to activity in AR 11040 mentioned earlier since the radio source is located close to the latter. Similarly, the intense discrete source above the solar limb in the northeast quadrant (Figure 3) is likely due to continued CME activity there.[5]

3. ANALYSIS AND RESULTS

The sudden changes in the radio emission from the Sun during a solar eclipse correspond to the covering (ingress) and/or uncovering (egress) of small areas of enhanced radio brightness in the solar atmosphere by the Moon's limb (Christiansen et al. 1949). At a typical frequency like 100 MHz, regions with angular dimensions as small as 15″ can be observed (see Equation (1)) as a result of the diffraction effects at the Moon's limb. This indicates that the "dip" in the 50 and 109 MHz time profiles in Figure 1 during the time interval ≈08:17–09:59 UT most likely corresponds to the occultation of discrete radio sources (located at the plasma levels corresponding to the above two frequencies) in the solar atmosphere by the Moon on 2010 January 15. We verified this by drawing the path of the Moon on the GRH image in Figure 3 using the time and P.A. information for the contact of the Moon with the optical Sun at various stages of the eclipse on 2010 January 15. The average rate of

[4] http://cdaw.gsfc.nasa.gov

[5] http://cor1.gsfc.nasa.gov/catalog/

movement of the Moon against the stellar background was taken to be $\approx 0\farcs3\ s^{-1}$ (Hazard 1976). The circles labeled 08:17 UT and 09:59 UT in Figure 3 indicate, respectively, the locations of the leading and trailing edge of the Moon's limb during the onset and end of the "dip" mentioned above. The duration of the "dip" (occultation) is ≈102 minutes. This is nearly the same as that for a central occultation (Hazard 1976). Therefore, the occulted sources must be close to the path of the center of the Moon. An inspection of Figure 3 suggests that the only possibility is the 50 and 109 MHz counterparts of the discrete radio source above the limb in the northeast quadrant. The latter also lies close to the two possible locations for the occulted source, i.e., the points of intersection of the circles representing the Moon's position at 08:17 UT and 09:59 UT. Note that the size of the sources could be smaller than what is noted in Figure 3 since the angular resolution of GRH is limited (see Section 2).

We calculated the angular size of the occulted sources, i.e., their linear extent in the direction of movement of the Moon, from the average of the time taken by the received solar flux to reach the minimum value (from the pre-occultation level) during the ingress and subsequently to reach the pre-occultation level from the minimum value during the egress (see Figure 1). The value is $\approx 1' \pm 0\farcs3$ at both 50 and 109 MHz. The plasma levels corresponding to the above frequencies are at different heights in the solar atmosphere. Therefore, the similarity in the source size at 50 and 109 MHz indicates that the cross-section of the associated coronal structure must be approximately constant as a function of radial distance, i.e., cylindrical-shaped. Here we have implicitly assumed that radio emission over the 109–50 MHz band originates at different heights from the same structure. Currently, there are two different views on the lateral dimension of radio-emitting structures in the solar corona: while some authors invoke cone-shaped diverging structures to explain their results (Sheridan et al. 1983; Thejappa & Kundu 1994), others use non-diverging cylindrical-shaped structures (Riddle 1974; Schmahl et al. 1994). The present observations with higher angular resolution seem to favor the latter. We would like to add here that the onset and end of the "dip" in Figure 1 are nearly the same at both 50 and 109 MHz. This indicates that the corresponding discrete radio sources were covered/uncovered by the Moon's limb at the same time. One possibility is that the associated cylindrical structure mentioned above might have been oriented along the line of sight to the observer.

Statistical studies reveal that the appearance of CMEs and the onset of radio noise storms are closely associated (Kerdraon et al. 1983; Kathiravan et al. 2007). Therefore, it is possible that the occulted radio source mentioned above is a noise storm since it is associated, both spatially and temporally, with a CME. We calculated its T_b at 77 MHz using the aforementioned angular size of $\approx 1'$, and the value is $\approx 3 \times 10^9$ K. This is about an order of magnitude higher than the previously reported maximum T_b of noise storm sources at low frequencies (Thejappa & Kundu 1991). Assuming that noise storm emission is circularly polarized (Elgarøy 1977), we calculated the possible coronal magnetic field (B_c) near the noise storm source region following the method described in Ramesh et al. (2011), and the value is ≈70 mG (corresponding to $T_b \approx 3 \times 10^9$ K). Note that the above value is at a radial distance $r \approx 1.3\ R_\odot$, the typical distance at which noise storm emission at 77 MHz occurs (Ramesh et al. 2011). If we presume that the observed noise storm emission is located in one of the "legs" of the CME or represents some other structural component of the CME as reported in the literature (Wild & Zirin 1956; McLean 1973; Lantos et al. 1981), the above estimate of B_c can be related to the associated CME in the present case. We could not verify this since the CME is noticeable only above $r > 2.2\ R_\odot$ in the coronagraph field of view owing to the presence of the occulting disk (Figure 4). We would like to point out here that Bird et al. (1985) had earlier estimated the magnetic field of a CME at a distance of $r \approx 2.5\ R_\odot$ (using combined white light and radio sounding observations) to be in the range 10–100 mG. Assuming that the B_c obtained using radio noise storms vary as $(r-1)^{-0.5}$ as derived by Ramesh et al. (2011), we find that the extrapolation of our estimate of ≈70 mG at $r \approx 1.3\ R_\odot$ in the present case gives ≈32 mG at $r \approx 2.5\ R_\odot$.

4. SUMMARY

Utilizing the annular solar eclipse of 2010 January 15 to observe the solar corona at low radio frequencies with much higher angular resolution than normally possible with the limited baselines of the telescopes, we find that the angular size of the smallest source observable in the frequency range 109–50 MHz is $\approx 1' \pm 0\farcs3$. The observed radio source was a noise storm continuum associated with a CME. Upon survey of the available literature, we find that this is the smallest coronal radio source size observed in the above frequency range. The estimated T_b based on the above source size is $\approx 3 \times 10^9$ K. Using the above value of T_b, we calculated the coronal magnetic field near the radio source region, and it is ≈70 mG. With the noise storms closely associated with CMEs and also usually circularly polarized, similar high angular resolution studies particularly in both total and circularly polarized intensity, are expected to be useful in understanding the CMEs close to the Sun where white light observations and magnetic field measurements are currently difficult. We would like to add here that although the smallest observed source size is $\approx 1'$ in the present case, it is possible that the observable limiting size of discrete radio sources in the solar corona, particularly frequencies $\lesssim$100 MHz, could be smaller still (McConnell 1983; Ramesh & Ebenezer 2001). The fact that the observed T_b ($\approx 3 \times 10^9$ K) in the present case is less than the predicted maximum T_b ($\approx 10^{10}$ K) for the noise storm continuum based on theoretical calculations (Thejappa 1991) supports this argument. In summary, our results quantitatively establish the usefulness and importance of low-frequency radio observations of the solar corona with subarcminute angular resolution.

The staff of the Gauribidanur Observatory are thanked for their help with data collection and maintenance of the antenna and receiver systems there. We profusely thank the referee for his/her comments, which helped us to present the results more clearly. The *SOHO* data are produced by a consortium of the Naval Research Laboratory (USA), Max-Planck-Institut für Aeronomie (Germany), Laboratoire d'Astronomie (France), and the University of Birmingham (UK). *SOHO* is a project of international cooperation between ESA and NASA. The *GOES* data were provided by the National Geophysical Data Center (NGDC).

REFERENCES

Bastian, T. S. 1994, ApJ, 426, 774
Bastian, T. S. 1995, ApJ, 439, 494
Bastian, T. S. 2004, Planet. Space Sci., 52, 1381
Benz, A. O., Grigis, P. C., Csillaghy, A., & Saint-Hilaire, P. 2005, Sol. Phys., 226, 121
Bird, M. K., Volland, H., Howard, R. A., et al. 1985, Sol. Phys., 98, 341

Brueckner, G. E., Howard, R. A., Koomen, M. J., et al. 1995, Sol. Phys., 162, 357
Cairns, I. H. 2004, Planet. Space Sci., 52, 1423
Christiansen, W. N., Yabsley, D. E., & Mills, B. Y. 1949, Aust. J. Phys., A2, 506
Cohen, M. H. 1969, ARA&A, 7, 619
Denisse, J.-F., Blum, E. J., & Steinberg, J.-L. 1952, Nature, 170, 191
Ebenezer, E., Subramanian, K. R., Ramesh, R., Sundararajan, M. S., & Kathiravan, C. 2007, Bull. Astron. Soc. India, 35, 111
Elgarøy, Ø. 1977, Solar Noise Storms (London: Pergamon)
Gergely, T. E. 1986, in Low Frequency Radio Astronomy, Proc. NRAO Workshop, ed. W. C. Erickson & H. V. Cane (Green Bank, WV: NRAO), 97
Hazard, C. 1976, in Methods of Experimental Physics, ed. M. L. Meeks (New York: Academic), 97
Kai, K. 1985, in Solar Radio Physics, ed. D. J. McLean & N. R. Labrum (Cambridge: Cambridge Univ. Press), 415
Kane, S. R., Kreplin, R. W., Martres, M.-J., Pick, M., & Soru-Escaut, I. 1974, Sol. Phys., 38, 483
Kassim, N. E., Polisensky, E. J., Clarke, T. E., et al. 2005, in ASP Conf. Ser. 345, From Clark Lake to the Long Wavelength Array: Bill Erickson's Radio Science, ed. N. E. Kassim, M. R. Pérez, W. Junor, & P. A. Henning (San Francisco, CA: ASP), 392
Kathiravan, C., Ramesh, R., Barve, I. V., & Rajalingam, M. 2011, ApJ, 730, 91
Kathiravan, C., Ramesh, R., & Nataraj, H. S. 2007, ApJ, 656, L37
Kerdraon, A. 1979, A&A, 71, 266
Kerdraon, A., Pick, M., Trottet, G., et al. 1983, ApJ, 265, L19
Kraus, J. D. 1966, Radio Astronomy (New York: McGraw-Hill)
Lang, K. R., & Willson, R. F. 1987, ApJ, 319, 513
Lantos, P., Kerdraon, A., Rapley, G. G., & Bentley, R. D. 1981, A&A, 101, 33
McConnell, D. 1983, Sol. Phys., 84, 361
McLean, D. J. 1973, Proc. Astron. Soc. Aust., 2, 222
Mercier, P., Subramanian, P., Kerdraon, A., et al. 2006, A&A, 447, 1189
Ramesh, R., & Ebenezer, C. 2001, ApJ, 558, L141
Ramesh, R., Kathiravan, C., & Satya Narayanan, A. 2011, ApJ, 734, 39
Ramesh, R., & Sastry, Ch. V. 2000, A&A, 358, 749
Ramesh, R., Subramanian, K. R., & Sastry, Ch. V. 1999, Sol. Phys., 185, 77
Ramesh, R., Subramanian, K. R., Sundararajan, M. S., & Sastry, Ch. V. 1998, Sol. Phys., 181, 439
Riddle, A. C. 1974, Sol. Phys., 35, 153
Robinson, R. D. 1983, Proc. Astron. Soc. Aust., 5, 208
Schmahl, E. J., Gopalswamy, N., & Kundu, M. R. 1994, Sol. Phys., 150, 325
Sheridan, K. V., Labrum, N. R., Payten, W. J., Nelson, G. J., & Hill, E. R. 1983, Sol. Phys., 83, 167
Subramanian, P., & Cairns, I. H. 2011, J. Geophys. Res., 116, A03104
Thejappa, G. 1991, Sol. Phys., 132, 173
Thejappa, G., & Kundu, M. R. 1991, Sol. Phys., 132, 155
Thejappa, G., & Kundu, M. R. 1994, Sol. Phys., 149, 31
White, S. M., Kassim, N. E., & Erickson, W. C. 2003, Proc. SPIE, 4853, 111
Wild, J. P., & Zirin, H. 1956, Aust. J. Phys., 9, 315